Mon. Not. R. Astron. Soc. **000**, 1–?? (2004) Printed 2 February 2008 (MN LATEX style file v2.2)

A multiply-imaged, submillimetre-selected ULIRG in a galaxy group at $z \sim 2.5$

Jean-Paul Kneib,[1,2] Paul P. van der Werf,[3] Kirsten Kraiberg Knudsen,[3] Ian Smail,[4] Andrew Blain,[1] Dave Frayer,[5] Vicki Barnard[6,7] & Rob Ivison[8]
[1] *Caltech-Astronomy, MC105-24, Pasadena, CA 91125, USA*
[2] *Observatoire Midi-Pyrénées, CNRS-UMR5572, 14 Avenue E. Belin, 31400 Toulouse, France*
[3] *Leiden Observatory, P.O. Box 9513, NL – 2300 RA Leiden, The Netherlands*
[4] *Institute for Computational Cosmology, University of Durham, South Road, Durham DH1 3LE, UK*
[5] *Caltech-SIRTF Science Center, MC220-06, Pasadena, CA 91125, USA*
[6] *Cavendish Astrophysics, University of Cambridge, Cambridge CB3 0HE*
[7] *Joint Astronomy Centre, 660 N. A'ohoku Place, Hilo, HI 96720, USA*
[8] *Astronomy Technology Centre, Blackford Hill, Edinburgh EH9 3HJ*

Received 2003 – –; Accepted: 2004 – –

ABSTRACT

We present observations of a remarkable submillimetre-selected galaxy, SMM J16359+6612. This distant galaxy lies behind the core of a massive cluster of galaxies, A 2218, and is gravitationally lensed by the foreground cluster into three discrete images which were identified in deep submillimetre maps of the cluster core at both 450 and 850μm. Subsequent follow-up using deep optical and near-infrared images identify a faint counterpart to each of the three images, with similar red optical–near-infrared colours and *HST* morphologies. By exploiting a detailed mass model for the cluster lens we estimate that the combined images of this galaxy are magnified by a factor of $\sim$45, implying that this galaxy would have un-lensed magnitudes $K_s = 22.9$ and $I = 26.1$, and an un-lensed 850-μum flux density of only 0.8 mJy. Moreover, the highly constrained lens model predicted the redshift of SMM J16359+6612 to be $z = 2.6 \pm 0.4$. We confirm this estimate using deep optical and near-infrared Keck spectroscopy, measuring a redshift of $z = 2.516$. SMM J16359+6612 is the faintest submm-selected galaxy so far identified with a precise redshift. Thanks to the large gravitational magnification of this source, we identify three sub-components in this submm galaxy, which are also seen in the NIRSPEC data, arguing for either a strong dust (lane) absorption or a merger. Interestingly, there are two other highly-amplified galaxies at almost identical redshifts in this field (although neither is a strong submm emitter). The three galaxies lie within a $\sim$ 100 kpc region on the background sky, suggesting this submm galaxy is located in a dense high-redshift group.

Key words: galaxies: individual: SMM J16359+6612 — galaxies: starburst — galaxies: evolution — galaxies: clusters: individual: A 2218 — infrared: galaxies — cosmology: observations

1 INTRODUCTION

Recent submillimetre (submm) surveys show that the majority of the submm background at wavelengths of $\sim 850\mu$m arises from a population of distant, highly luminous infrared galaxies with 850 μm flux densities of $\gtrsim 1$ mJy (Blain et al. 1999; Cowie et al. 2002; Smail et al. 2002). The steep slope of the submm counts indicates that the integrated background is dominated by ~ 1 mJy galaxies, below the ~ 2 mJy confusion limit of the deepest blank-field 850μm surveys carried out to date (Hughes et al. 1998), and well below the 3–8 mJy flux density limits (3–4σ) typically achieved in wider-field 850 μm surveys (e.g. Eales et al. 1999; Scott et al. 2002; Webb et al. 2003).

Submm galaxies in the 1-mJy regime can, however, only be studied at present by exploiting a natural telescope – a massive gravitational lens formed by a rich clusters of galaxies – which provide the opportunity of overcoming both the confusion limit (by spatially magnifying an area of the sky behind the lens) and the sensitivity limit (by gravitational

magnification of the sources within this area). This strategy has successfully been used by Smail, Ivison & Blain (1997), Chapman et al. (2002), Cowie et al. (2002) and Smail et al. (2002) to detect submm sources amplified by factors typically of 1.5–4×. Unfortunately, the intrinsically faintest sources are usually only detected at modest significance, complicating the identification and analysis of their counterparts in other wavebands.

To investigate the properties of the mJy-population in detail we require a high-signal-to-noise detection of a sub-mJy submm galaxy. Such systems can arise in rare configurations where the source is located within a small region on the background sky defined by the caustic of the lens, which then forms multiple, highly magnified images of the background galaxy (see also Borys et al. 2004). This situation not only provides a tool for investigating the properties of intrinsically faint galaxies in detail, but also provides a unique opportunity to measure the redshift of the background galaxy from the geometry of the images combined with an accurate model of the cluster lens, using a ray-tracing technique to triangulate the three-dimensional position of the galaxy in the volume behind the lens. This technique, which was demonstrated successfully by Kneib et al. (1996) and confirmed by Ebbels et al. (1998), circumvents the need for bright optical or infrared counterparts to a submm galaxy prior to measuring its redshift. We may thus avoid a bias in redshift measurements towards unrepresentative, low redshift or less obscured systems (Smail et al. 2002; Webb et al. 2003).

This paper describes the discovery of a multiply-imaged submm galaxy, SMM J16359+6612, which is gravitationally lensed by the core of the rich cluster A 2218, and appears as three distinct sources in our 850 μm discovery map. We identify faint counterparts to all three sources in deep optical and near-infrared (NIR) imaging, consistent with their identification as three images of a single background galaxy. We estimate its redshift using a detailed mass model for the cluster lens. We then confirm the accuracy of the redshift with spectroscopic observations and finally discuss the intrinsic properties of this system. Throughout we will assume an $\Omega = 0.3$, $\Lambda = 0.7$ cosmology with $H_0 = 70\,\mathrm{km\,s^{-1}\,Mpc^{-1}}$. At a redshift of $z = 2.516$ the angular scale is thus 8.06 kpc/arcsec.

2 OBSERVATIONS AND RESULTS

2.1 Submillimetre imaging

We used the Submillimetre Common User Bolometer Array (Holland et al. 1999) on the 15-m James Clerk Maxwell Telescope (JCMT) in March 1998 and in August 2000 to image a 2.3′ diameter field centred on the core of the $z = 0.17$ cluster A 2218. Total time on source excluding overheads was 95 ks at a wavelength of 850 μm with chop-throws of 45 and 90″ at a variety of position angles. During the best observing conditions data were also collected at 450 μm (72 ks in total without overheads). Zenith opacities varied from 0.15 to 0.4 at 850 μm and from 0.6 to 1.0 at 450 μm. Pointing was monitored and corrected every hour, and was found to be accurate to better than 3″. The data were reduced using the SURF package (Jenness & Lightfoot 1998). Data reduction steps consisted of flat-fielding the demodulated data, opacity correction, despiking, flagging bad integrations, pointing correction, sky subtraction using the least noisy bolometers, and rebinning onto a 1″ grid, weighting the bolometers with the inverse variances of their signals. Flux calibration was achieved using maps of Uranus, and absolute flux calibration should be accurate to approximately 10% at 850 μm and 20% at 450 μm, as derived from the consistency of the calibration measurements. The resulting 850 μm image was convolved with a 5″ Gaussian to remove high-frequency noise and subsequently deconvolved using a CLEAN algorithm (Hogbom 1974), in order to remove the negative sidelobes resulting from the small chop throw that was used for these data. After restoration with a 15″ full width at half maximum (FWHM) Gaussian beam the resulting image has an r.m.s. noise of approximately $1.5\,\mathrm{mJy\,beam^{-1}}$.

2.2 Optical and Near-infrared imaging

The optical images come from the *Hubble Space Telescope* (*HST*) WFPC2 Early Release Observations made after the SM-3a servicing mission in January 2000. The dataset consists of 6 orbits in both F450W (11.0 ks) and F814W (12.0 ks) and 5 orbits in F606W (10.0 ks). The reduction of these images is described in Smail et al. (2001). The final WFPC2 frames have a FWHM of 0.17″ and 3-σ point source sensitivities of B_{450} =28.8, V_{606} =29.0 and I_{814} =28.1 in the Vega-based system from Holtzman et al. (1995).

The NIR imaging used in our analysis was obtained with the INGRID camera (Packham et al. 2003) on the 4.2-m William Herschel Telescope (WHT). The observations were obtained during INGRID commissioning on March 22 and 23, 2000. The dataset consists of a total of 9.1 ks integration in K_s and 8.3 ks in J-band obtained under photometric conditions in 0.6–0.8″ seeing. More details on the reduction of these data is described by Smail et al. (2001). The absolute calibration is accurate to approximately 0.03 mag. The final coadded frames have 3-σ point source sensitivities, within the seeing disk, of K_s =22.0 and J =23.7, and seeing of 0.75″.

2.3 Source Identification

We overlay the 850 μm image on a true colour representation of the cluster core in 1. Both the 850 and 450μm SCUBA images show a number of bright submm sources located in the saddle region in the cluster core, formed by the two brightest cluster members. At 850 μm, at least four sources are readily identified above the 5-σ detection limit of ~ 8 mJy. From North to South these are SMM J16359+6613 ($\alpha = 16^h35^m55.625^s$, $\delta = +66^d12^m59.5^s$), SMM J16359+6612.6, SMM J16359+6612.4 and SMM J16358+6612.1 (Table 1). The latter three sources also appear in the 450 μm map, but the northern source is not detected at 450 μm. Significantly, the 450/850 μm flux ratios for the three southern sources are identical within the errors, 4.0 ± 0.4. In contrast, the northern source has a 3-σ limit of $S_{450}/S_{850} \leqslant 1.6$.

Inspecting the positions of the four submm sources in the optical and NIR data, we identify unusually red objects close to the position of all three southern submm sources, while the field of the northern submm source,

see JPEG file a2218smm.jpg

Figure 1. (Left) A true-colour image of the core of A 2218 composed from the *HST* F450W (blue), *HST* F814W (green) and WHT/INGRID K_s (red) images. The 850 μm submm image from SCUBA is overlayed as white contours at flux densities of 2.5, 3.3, 5.0, 6.6, 8.3, 10 mJy beam^{-1}. The three images of the multiply-imaged submm galaxy are annotated as A, B and C. We also identify the 2 other galaxies at $z \sim 2.5$, namely the single-image #273 and the fold-image #384 and its counter-image #468. The yellow line shows the critical line at $z = 2.515$. (Right) Panel of $10'' \times 10''$images showing the INGRID K_s-band (left column) and *HST* true colour image from F450W/F606W/F814W (right column) of the four submm sources in the core of A 2218. The resolution of these frames is $\sim 0.75''$ and $\sim 0.15''$ respectively. The K-band panels are centered on the submm source, and the colour HST panels are centered on the identified optical counterpart. The contours on the K_s frames show the morphologies of the galaxy in the F814W passband at the resolution of the K_s-band frame. Note how each of the submm sources, SMM J16359+6612.6, SMM J16359+6612.4 and SMM J16358+6612.1, comprises a NIR source (γ) which is bracketed by two features in the F814W image (α and β). The morphological and photometric similarity of these three objects suggests that they are all images of the same background source. For SMM-A and SMM-B we have indicated in their *HST* true colour image the extent of the Hα line observed in the NIRSPEC data (white segments). Note that there is a very faint red counterpart for the SMM J16359+6613 in the F814W image that does not appear in the K-band data, and that all the bright galaxies near SMM-B and SMM-C are spectroscopically confirmed cluster members (SMM-B is next to a star forming galaxy, and SMM-C is next to three elliptical galaxies). In all the images North is up and East is to the left.

Table 1. Properties of SMM J16359+6612. All optical and NIR magnitudes are measured in a $2''$diameter apertures (Smail et al. 2001). The position relative to the centre of the cD galaxy (at $16^h35^m49.21^s$, $66^d12^m44.7^s$, J2000) was computed from the K_s-band data and has a relative uncertainty of $\pm 0.5''$. None of these sources is detected in the *ISO* image on A2218 with a 3-σ upper limit of 0.11 μJy (Metcalfe et al. 2003). Flux density measurements and magnitudes in this table have not been corrected for gravitational magnification.

ID	$\Delta\alpha$ ($''$)	$\Delta\delta$ ($''$)	$B-I$	$V-I$	$I-K$	$J-K_s$	K_s	f_{450} mJy	f_{850} mJy	f_{450}/f_{850}	Amp
A	35.6	−7.3	1.10 ± 0.05	0.45 ± 0.05	3.00 ± 0.1	1.2 ± 0.2	20.2 ± 0.1	45 ± 9	11 ± 1	4.0 ± 0.9	14 ± 2
B	29.6	−21.1	1.07 ± 0.05	0.41 ± 0.05	3.67 ± 0.1	2.7 ± 0.2	19.5 ± 0.1	75 ± 15	17 ± 2	4.4 ± 1.0	22 ± 2
C	10.2	−39.1	1.37 ± 0.15	0.30 ± 0.15	3.25 ± 0.1	2.0 ± 0.2	20.5 ± 0.1	32±6	9 ± 1	3.6 ± 0.8	9 ± 2
#468	-25.7	−21.8	1.25 ± 0.05	0.53 ± 0.05	2.82 ± 0.1	1.4 ± 0.1	20.0 ± 0.1	—	—	—	6 ± 1
#273	40.3	−20.7	0.85 ± 0.05	0.28 ± 0.05	0.75 ± 0.1	0.0 ± 0.1	20.9 ± 0.1	—	—	—	30 ± 5

SMM J16359+6613, shows a faint red counterpart visible in the *HST/F814W* frames but undetected in the ground-based K_s-band image. We show the relevant regions of the INGRID K_s and *HST* frames in Figure 1. It is worth noting that for all three southern sources the relative astrometric offsets between the K_s-band counterpart and the 850 μm peak is less than $2''$.

We label the optical/NIR counterparts to the three southern submm sources from North to South: SMM-A (SMM J16359+6612.6), SMM-B (SMM J16359+6612.4), and SMM-C (SMM J16358+6612.1) and list the photometry for these within matched apertures from our optical and NIR frames in Table 1. The colours of the three counterparts are similar, although crowding in the various fields and the effects of differential amplification on our fixed-aperture photometry may explain the lack of precise agreement (the colours of SMM-A should give the best indication of the true spectral energy distribution of the galaxy as it is not contaminated by any foreground galaxy). Nevertheless, all three counterparts show a similar pattern of a pronounced red core surround by two blue regions, for example in SMM-B the centre of the galaxy (γ) is much brighter in K_s than in I_{814}, while the southern (and northern) extremities, α and β, are considerably brighter in I_{814} (Figure 1). A similar pattern of a red centre bracketed by bluer regions is seen in SMM-A and C. We illustrate that this effect is not a result of the different spatial resolutions of the K_s and I_{814} frames by contouring the seeing-matched I_{814} over the K_s-band frame in Figure 1.

The photometric similarity of the three southern submm sources, combined with the fact that their counterparts exhibit strong spectral and morphological similarities, suggests that we are seeing three images of a single luminous submm galaxy (which we will call SMM J16359+6612 in the following), lying behind the cluster. The configuration, relative brightnesses and parities of the three images are consistent with the predictions of a detailed mass model of the cluster core (Kneib et al. 1996). With the assumption that these submm sources are three multiple images of a unique galaxy, we can predict a redshift of $z = 2.6 \pm 0.4$ using the lens model of Kneib et al. (1996) updated to include a recently discovered $z = 5.56$ lensed galaxy (Ellis et al. 2001). For comparison, the 450/850μm flux ratio for this galaxy corresponds to a redshift/dust temperature value $(1+z)/(T/40\mathrm{K}) = 3.2 \pm 0.3$ (Blain et al. 2002) or a redshift range of $z = 1.9$–4.5 from the spectral energy distributions models in Hughes et al. (1998).

2.4 Keck spectroscopy

On June 30 and July 1st 2003, we conducted deep multi-slit spectroscopy with the Low Resolution Imaging Spectrograph (LRIS; Oke et al. 1995), of sources lying in the field of the rich cluster A 2218 (see Kneib et al. 2004 for a complete description of these data and a detailled discussion of the mass model). The two nights had reasonable seeing, $\sim 0.8''$, but were not fully photometric (with some cirrus), nevertheless we obtained a crude flux calibration of our observations using Feige 67 and 110 as spectrophotometric standard stars.

We observed the SMM-A source for a total of 10.6 ks using the 600/4000 blue grism and the 400/8500 red gratings offering respectively a spectral dispersion of 0.63Å pixel^{-1}

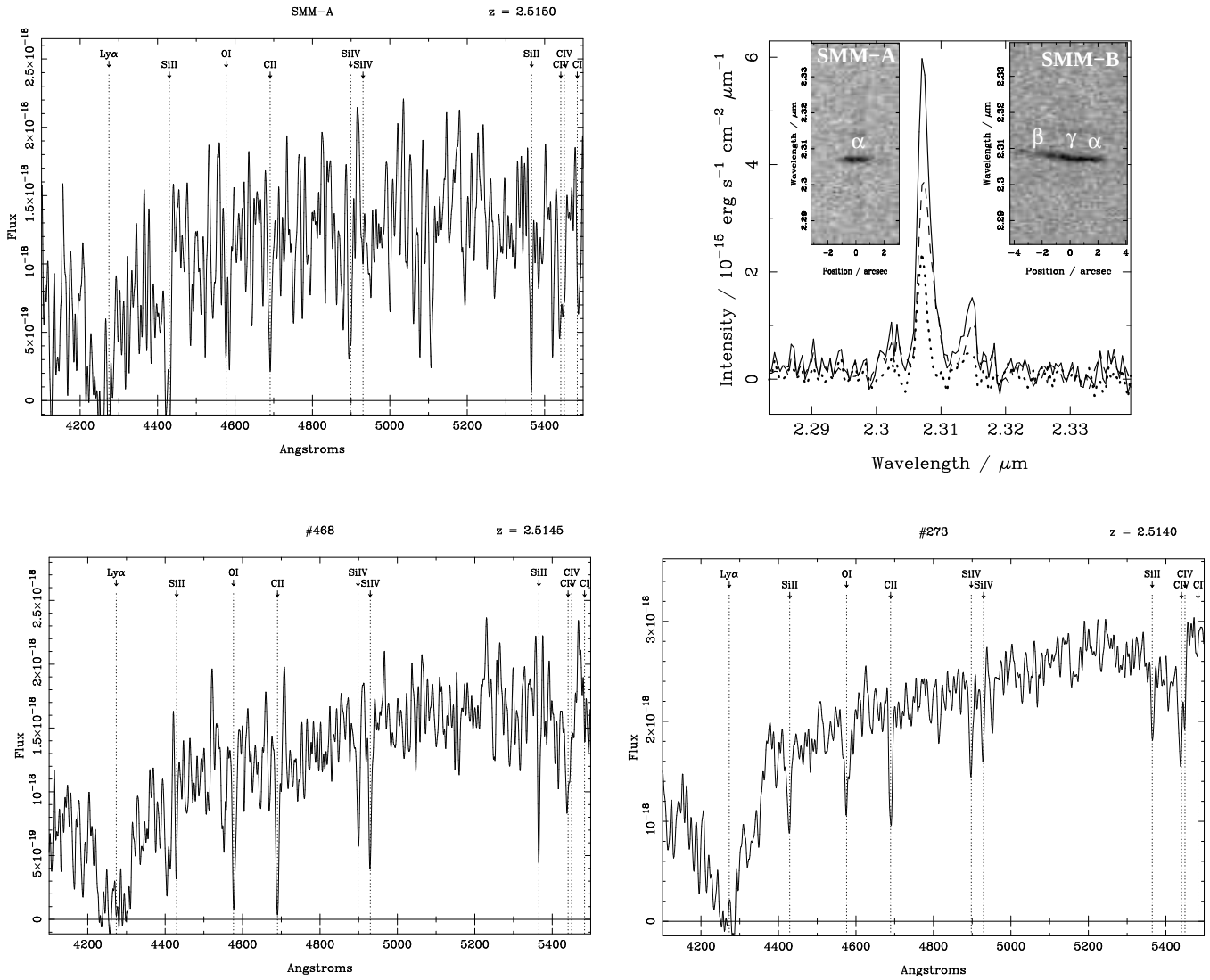

Figure 2. Spectroscopic identification of the three $z \sim 2.515$ galaxies behind A 2218 from our blue-arm LRIS spectra: (*Top-Left*) SMM-A, (*Bottom-Left*) #468 and (*Bottom-Right*) #273. Note the similar UV fluxes of the three galaxies, even though they have very different submm luminosities, and by implication very different total star formation rates. The three spectra have been rebinned to the same spectral resolution of 2Å and the wavelength scale is in the observed frame. The flux is given in units of erg s^{-1} cm^{-2} Å^{-1}. *Top-Right:* Keck/NIRSPEC K-band spectrum of SMM-A (dotted), SMM-B (dashed) and the sum of SMM-A and B (solid) showing the redshifted Hα and NII emission lines. The inset shows the 2-d region of the spectrum around the Hα line in SMM-A and SMM-B demonstrating the extended spatial morphology of the emission line in both images and the presence of a gravitationally amplified velocity gradient within SMM-B. e annotated the Hα line with the position of the different sub component of the galaxy (α, β and γ).

in the blue and 1.86Å pixel^{-1} in the red. We included in the same mask a slitlet on the galaxy #468 (the counter image of the $z = 2.515$ fold arc #384: Ebbels et al. (1996), see also Le Borgne et al. (1992)). The spectra of SMM-A and #468 both show strong Ly-α absorption and numerous metal lines (Figure 2). The derived redshift for SMM-A is 2.515 ± 0.001 based on the strongest interstellar absorption lines: OIλ1302.17Å and CIIλ1334.5Å as well as CIVλ1548.19 and 1550.77 in absorption. These observations also yielded a redshift for #468 of 2.5145 ± 0.001.

In addition, a 9.2-ks exposure using the 400/3400 blue grism on a second mask targeting galaxies in this field yielded a redshift for another $z \sim 2.5$ galaxy. This galaxy is identified as #273 (Le Borgne et al. 1992) and was misidentified as a $z = 0.800$ galaxy by Ebbels et al. (1998) who confused the CIII]λ1908.7Å emission line with [OII]λ3727Å. As for SMM-A and #384/#468, #273 shows prominent Ly-α absorption and many metal absorption lines from which we derived a redshift of 2.514 ± 0.001 (Figure 2). All three galaxies are thus within 100 km s^{-1} of each other in the rest frame (ignoring uncertainties due to possible velocity offsets in the UV lines we use). Figure 2, shows the UV spectra of all three galaxies with the identified absorption lines.

The counterparts of the submm sources SMM-A and SMM-B were also independently targeted in the K-band using the NIR spectrograph NIRSPEC on Keck II (McLean et al. 1998). These observations were obtained in 2002 August 18 in non-photometric conditions and 0.6″ seeing. Eight exposures of 600 s each were obtained, nodding along the 0.76″×42″ slit by 8″ between each exposure. Sources A and

B were on the slit simultaneously. Wavelength calibration was achieved from the sky lines, using observations of a bright star to correct for geometrical distortion. An average sky spectrum was created by scaling and combining the individual spectra, and this was then subtracted from each science observation before co-adding and extracting the spectra. Approximate flux calibration and telluric absorption correction was achieved using an observation of UKIRT standard stars from the previous night. No attempt was made to correct for slit losses.

The flux-calibrated spectrum (Figure 2) reveals three emission lines identified as Hα and the two weaker flanking [NII] lines. The Hα line extends over 2.2″ for SMM-A and 5.1″ for SMM-B, which compares well with the optical size of α in SMM-A and the total extent of α, γ and β for SMM-B as shown in the *HST* panels in Figure 1 and the two insets in Figure 2. There are hints in SMM-A for a more compact distribution of [NII] emission. The Hα line is centered on 2.30755μm placing the submm galaxy at a redshift of $z = 2.5165 \pm 0.0015$, indicating that the UV interstellar lines used to derive a redshift in the optical are blueshifted by $\sim 100\,\mathrm{km\,s^{-1}}$ with respect to the systemic velocity of the galaxy. The restframe width of the Hα line corresponds to $\sim 280 \pm 60\,\mathrm{km\,s^{-1}}$, and there is a hint of coherent velocity structure in the spectrum of SMM-B, with a velocity shift of about $220 \pm 60\,\mathrm{km\,s^{-1}}$ over an angular distance of 2.6″ (~ 1.5 kpc in the source plane). The fact that we do not see such structure in the SMM-A image is due to the fact that only component α (and probably part of γ) was in the NIRSPEC slit. Hence, this velocity shift could argue that the complex optical/NIR morphology of this source is best explained by a strong dust absorption in a rotating disk structure or better by a merger.

The total Hα line flux for the combined spectra of SMM-A and B is $f_{H\alpha} = 2.7 \times 10^{-20}\,\mathrm{W\,m^{-2}}$, with a ratio of 2.3 between their respective Hα flux densities. This corresponds to a Hα luminosity $L_{\mathrm{H}\alpha} = 3.7 \times 10^8\,\mathrm{L_\odot}$, or a (unlensed) star-formation rate of $11\,\mathrm{M_\odot\,yr^{-1}}$. The narrow width of the Hα emission line and the observed ratio of NII/Hα (0.3 ± 0.1) suggest that the emission is dominated by star formation, with little evidence for a strong AGN.

3 RESULTS AND DISCUSSION

The occurrence of a submm galaxy falling within the caustic lines of a massive foreground gravitational lens provides unique constraints on the properties of this faint submm galaxy. Using the cluster mass model we estimate that the background galaxy is gravitationally amplified by a factor of ∼45 (integrated across all three images), indicating that the intrinsic 850 μm flux density of this galaxy would be 0.8 mJy in the absence of gravitational magnification, while in the optical and NIR the galaxy would have magnitudes $I_{814} = 26.1$ and $K_s = 22.9$. The galaxy therefore represents a serendipitously positioned example of the submm galaxy population at flux levels of ~ 1 mJy, the population which produces the bulk of the submm background (Blain et al. 1999). This provides a unique opportunity to compare the properties of this low-luminosity submm galaxy with those of more luminous, submm galaxies studied in brighter, blank-field surveys (e.g. Ivison et al. 2002; Chapman et al. 2003).

A second, multiply-imaged submm galaxy has been identified by Borys et al. (2004), giving two high-magnification examples from the 24 cluster lenses at $z > 0.1$ mapped with sufficient sensitivity using SCUBA (Chapman et al. 2002; Smail et al. 2002; Knudsen et al. in prep.). The surface density of $\geqslant 1$ mJy submm galaxies is around $3\,\mathrm{arcmin^{-2}}$ (Smail et al. 2002; Cowie et al. 2002), suggesting that roughly ten clusters need to be surveyed to detect a strongly-lensed mJy-flux submm galaxy. This is consistent with the expectation based on models for the cluster lenses of uniform $\sim 800\,\mathrm{km\,s^{-1}}$ potential wells at $z \sim 0.2$, each with a critical curve encircling $0.05\,\mathrm{arcmin^{-2}}$, and background submm galaxies at $z \sim 2.4$ (see Kraiberg et al 2004 for a thorough discussion).

In our assumed cosmology the far-infrared luminosity of SMM J16359+6612 is $1.0 \times 10^{12}\,\mathrm{L_\odot}$, roughly 1.5× fainter than Arp 220, close to the border-line between luminous infrared galaxies and ultraluminous infrared galaxies (ULIRGs). The star formation rate derived from the far-infrared luminosity is about $500\,\mathrm{M_\odot\,yr^{-1}}$. Figure 3 compares the restframe (lens-corrected) SED of the SMM J16359+6612 to the SEDs of Arp 220, the well-studied $z = 2.8$ submm galaxy SMM J02399−0136 and the $z = 1.44$ Extremely Red Object and submm galaxy HR10 (Dey et al. 1999). The $\mathrm{L}_{FIR}/\mathrm{L}_{opt}$ ratio is higher than that seen for Arp 220, suggesting it is more obscured, and similar to the high-redshift, but much more luminous, SMM J02399−0136 (Ivison et al. 1998).

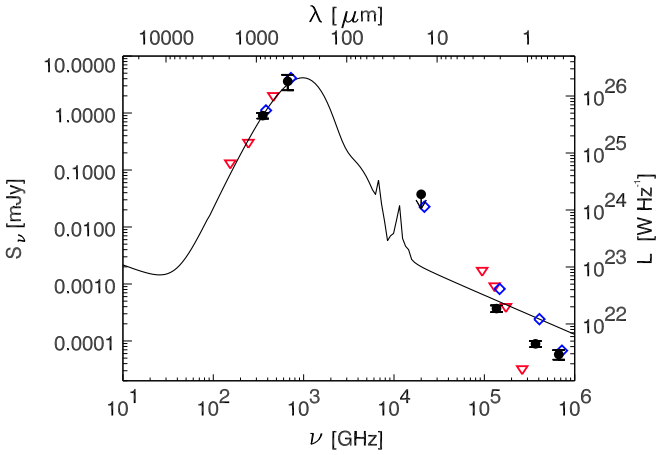

FIG. 4. — The observed Spectral Energy Distribution (SED) of the multiply-imaged submm galaxy SMMJ 16359+6612 (solid points with error bars) compared to Arp 220 (solid line, composite spectrum from Anantharamaiah et al. 2000, Klaas et al. 1997, Lisenfeld et al. 1996 and Surace et al. 2000) which is 1.5× more luminous in the far-infrared, as well as the well-studied submm galaxy SMMJ 02399−0136 (open diamonds, at $z = 2.8$, Ivison et al. 1998) which is 10× more luminous in the far-infrared, and the Extremely Red object HR10 (open triangles, at $z = 1.44$, Dey et al. 1999) which is 7× more luminous in the far-infrared. All SEDs are redshifted to match that of SMM J16359+6612 and scaled so they have a similar far-infrared luminosity. Notice the relatively large variation of $\mathrm{L}_{FIR}/\mathrm{L}_{opt}$ between the different galaxies.

At $z = 2.515$ the spatial resolution of the *HST* images,

corresponds to ~ 0.1 kpc, taking into account the gravitational magnification. Thus the colour gradient within the background galaxy is on 1–2 kpc scales – similar to the obscured region in nuclear starbursts in ultraluminous infrared galaxies at the present-day. A constraint on the size of the submm emission region is obtained by subtracting point sources from the 850 and 450 μm maps. This procedure leaves no detectable residual of extended emission, indicating that to our measurement accuracy we are dealing with point sources. The tightest constraint is obtained at 450 μm where we find that the intrinsic extent of the emission is less than $4''$, which corresponds to ~ 8 kpc. There is thus no indication for a highly extended obscured starburst in this relatively low-luminosity submm galaxy.

The precise redshift we have measured for SMM J16359+6612 enables us to identify that this galaxy lies at an identical redshift to that of #273 and the #384/#468 multiple image system. Using the lens model we estimate that SMM J16359+6612 lies between the #384/#468 and #273 galaxies in the source plane, and all three galaxies are less than 130 kpc apart. If these galaxies were not magnified by the cluster lens, all three galaxies would appear within a radius of $8''$. Moreover, we can place a limit of $\lesssim 100\,\mathrm{km\,s^{-1}}$ on the possible velocity offset between these three galaxies. They are thus all part of a single group and it is likely that they are interacting, which may explain the activity we detect in the submm waveband. The strong clustering of the submm galaxies with UV-bright populations highlights the opportunity for measuring the distances to submm galaxies from the redshifts of less-obscured companions, as well as the possible confusion which may arise when trying to relate UV- and submm-selected populations, in the absence of precise positions from radio counterparts.

SMM J16359+6612 has much redder colour in $(V-I)$ and $(I-K)$ than the two other nearby UV-selected galaxies, confirming the dustier nature of this galaxy. If we compare the unlensed star formation rate (SFR) for this three systems, we find based on their UV continuum that: SMM J16359+6612 has 6 $\mathrm{M_\odot\,yr^{-1}}$ (although certainly underestimated due to dust extinction) #468: 14 $\mathrm{M_\odot\,yr^{-1}}$ and #273: 4 $\mathrm{M_\odot\,yr^{-1}}$. For SMM J16359+6612 we can compare the three estimates of its amplification-corrected star formation rate: 6 $\mathrm{M_\odot\,yr^{-1}}$ from its dust-corrected UV luminosity, 11 $\mathrm{M_\odot\,yr^{-1}}$ from the Hα flux (uncorrected for extinction or aperture losses) and 500 $\mathrm{M_\odot\,yr^{-1}}$ based on the far-infrared emission. Applying the median extinction correction derived for mid-IR selected luminous infrared galaxies at $z \sim 0.7$ by Flores et al. (2003), $\mathrm{A_{H\alpha}} \sim 2.1$, and a modest correction for slit losses would increase the Hα-derived star formation rate by a factor of $\sim 10\times$. These results suggest the vast majority of the young stars in this galaxy are obscured by dust and are undetectable in the restframe far-UV. Although it is $10\times$ less luminous than the typical submm-selected galaxy studied in blank-field surveys, this system shares the same extreme levels of obscuration seen in the more luminous galaxies, rather than the more modest dust obscuration inferred for the somewhat less luminous UV-selected galaxies at these redshifts. We also note that the Hα line width and velocity structure, if they reflect the dynamics of the galaxy, suggest that this system is more massive for its UV luminosity than typical UV-selected galaxies at this epoch (Erb et al. 2003).

In summary, we have identified a multiply-imaged submm galaxy seen through the core of the rich cluster A 2218. The cluster lens amplifies the background galaxy by a factor of $\sim 45\times$, providing a high signal-to-noise view of an example of the sub-mJy submm population which provides the bulk of the extragalactic background in this waveband. We estimate a redshift for this galaxy from our highly-constrained lens models for the cluster and confirm this using optical and near-infrared spectroscopy from Keck. The redshift of the submm galaxy is $z = 2.516$, placing it at the same redshift as two other strongly-lensed UV-bright galaxies in this field. Our Keck spectroscopy suggests that the emission from the submm galaxy is dominated by star formation and in contrast to the typical UV spectral properties of more luminous submm galaxies, this galaxy shows Ly-α absorption, rather than emission (c.f. Chapman et al. 2003). The star formation rates we derive from the UV continuum, Hα and far-infared emission show that most of the star formation activity is obscured and we suggest it is likely to be located in the component γ, given its extreme $(I-K)$ colour. Because of its faint submm flux this galaxy is likely to be a good example of the type of galaxy that makes most contribution to the star formation history, thus deserving a detailled study with submm/mm interferometer to study the dynamics and mass of this obscured region. The presence of three highly-amplified $z = 2.515$ galaxies in our survey field indicates that the submm galaxy resides in a compact group, interactions within which may help explaining the triggering of the obscured starburst we detect.

ACKNOWLEDGEMENTS

We are grateful to R. Blandford, A. Fruchter, R. Hook, C. Packham, J. Peacock, N. Reddy, G. Smith, R. Tilanus and T. Treu for their respective roles in the acquisition and reduction steps for the data that this paper is based upon. We thank the anonymous referee for his constructive and useful report. JPK acknowledges support from CNRS and Caltech. IRS acknowledges support from the Royal Society and the Leverhulme Trust. AWB acknowledges support from the NSF under grant number AST-0205937. We also acknowledge support from the UK–French ALLIANCE collaboration programme #00161XM. The JCMT is operated by the Joint Astronomy Centre on behalf of the United Kingdom Particle Physics and Astronomy Research Council (PPARC), the Netherlands Organization for Scientific Research, and the National Research Council of Canada. Some of this data was obtained at the W. M. Keck Observatory, operated as a scientific partnership among Caltech, the University of California and NASA. The Observatory was made possible by the generous financial support of the W. M. Keck Foundation. The William Herschel Telescope is operated on the island of La Palma by the Isaac Newton Group in the Spanish Observatorio del Roque de los Muchachos of the Instituto de Astrofisica de Canarias. This paper is based on observations obtained with the NASA/ESA *Hubble Space Telescope*, obtained from the Data Archive of the Space Telescope Science Institute which is operated by the Association of Universities for Research in Astronomy, Inc., under NASA contract NAS5-26555.

REFERENCES

Anantharamaiah K., Viallefond F., Mohan N., Goss W., Zhao J., 2000, ApJ, 537, 613
Blain A., Kneib J.-P., Ivison R., Smail I., 1999, ApJ, 512, L87
Blain A., Smail I., Ivison R.J., Kneib J.-P., Frayer D.T., 2002, Physics Reports, 369, 111
Borys C., Chapman, S., Donahue, M., Fahlman G., Halpern M., Kneib J.-P., Newbury P., Scott D., Smith G.P., 2004, MNRAS, submitted
Chapman S. C., Scott, D., Borys, C., Fahlman, G. G., 2002, MNRAS, 330, 92
Chapman S. C., Blain A. W., Ivison R. J., Smail I., 2003, Nature, 422, 695
Dey A., Graham J. R., Ivison R. J., Smail I., Wright G. S., Liu M. C., 1999, ApJ, 519, 610
Cowie L. L., Barger A. J., Kneib J.-P., 2002, AJ, 123, 2197
Eales S., Lilly S., Gear W., Dunne L., Bond J., Hammer F., Le Fèvre O., Crampton D., 1999, ApJ, 515, 518
Ebbels T., Ellis R., Kneib J.-P., Leborgne J.-F., Pello R., Smail I., Sanahuja B., 1998, MNRAS, 295, 75
Ebbels T., Le Borgne J.-F., Pello R., Ellis R., Kneib J.-P., Smail I., Sanahuja B., 1996, MNRAS, 281, L75
Ellis R., Santos M., Kneib J.-P., Kuijken K., 2001, ApJ, 560, L119
Erb D., Shapley A., Steidel C., Pettini M., Adelberger K., Hunt M., Moorwood A., Cuby J.-G., 2003, ApJ, 591, 101
Flores, H., et al., 2003, A&A, in press.
Klaas U., Haas M., Heinrichsen I., Schulz B., 1997, A&A, 325, L21
Kneib J.-P., Ellis R., Smail I., Couch W., Sharples R., 1996, ApJ, 471, 643
Kneib et al. 2004 in preparation
Jenness T., Lightfoot J. F., 1998, adass, 7, 216
Lisenfeld U., Isaak K. G., Hills R., 2000, MNRAS, 312, 433
Holland W. S. et al., 1999, MNRAS, 303, 659
Holtzman J., Burrows C., Casertano S., Hester J., Trauger J., Watson A., Worthey G., 1995, PASP, 107, 1065
Hughes D. H. et al., 1998, Natur, 394, 241
Ivison, R. J., et al., 2002, MNRAS, 337, 1
Ivison, R. J., Smail, I., Le Borgne, J.-F., Blain, A. W., Kneib, J.-P., Bezecourt, J., Kerr, T. H., Davies, J. K., 1998, MNRAS, 298, 583
LeBorgne J. F., Pello R., Sanahuja B., 1992, A&AS, 95, 87
McLean I. S. et al., 1998, SPIE, 3354, 566
Metcalfe L., et al., 2003, A&A, 407, 791
Packham C., et al., 2003, MNRAS, 345, 395
Oke J. B. et al., 1995, PASP, 107, 375
Scott, S. E., et al., 2002, MNRAS, 331, 817
Smail I., Ivison R. J., Blain A. W., Kneib J.-P., 2002, MNRAS, 331, 495
Smail I., Kuntschner H., Kodama T., Smith G. P., Packham C., Fruchter A., Hook R., 2001, MNRAS, 323, 839
Smail I., Ivison R. J., Blain A. W., 1997, ApJ, 490, L5
Surace J. A., Sanders D. B., Evans A. S., 2000, ApJ, 529, 170
Webb T. M., et al., 2003, ApJ, 582, 6

This figure "a2218smm.jpg" is available in "jpg" format from:

http://arXiv.org/ps/astro-ph/0403192v1